Computational and Structural Biotechnology Journal 21 (2023) 3854–3864

Contents lists available at ScienceDirect

Computational and Structural Biotechnology Journal

journal homepage: www.elsevier.com/locate/csbj

Calcineurin B inhibits calcium oxalate crystallization, growth and aggregation via its high calcium-affinity property

Sudarat Hadpech, Sakdithep Chaiyarit, Visith Thongboonkerd *

Medical Proteomics Unit, Research Department, Faculty of Medicine Siriraj Hospital, Mahidol University, Bangkok, Thailand

ARTICLE INFO

Keywords:
Calcineurin inhibitor
Cyclosporin
EF-hand
FK506
Kidney stone
Stone inhibitor
Tacrolimus
Urolithiasis

ABSTRACT

Calcineurin inhibitors (CNIs) are widely used in organ transplantation to suppress immunity and prevent allograft rejection. However, some transplant patients receiving CNIs have hypocitraturia, hyperoxaluria and kidney stone with unclear mechanism. We hypothesized that CNIs suppress activities of urinary calcineurin, which may serve as the stone inhibitor. This study aimed to investigate effects of calcineurin B (CNB) on calcium oxalate monohydrate (COM) stone formation. Sequence and structural analyses revealed that CNB contained four EF-hand (Ca^{2+}-binding) domains, which are known to regulate Ca^{2+} homeostasis and likely to affect COM crystals. Various crystal assays revealed that CNB dramatically inhibited COM crystallization, crystal growth and crystal aggregation. At an equal amount, degrees of its inhibition against crystallization and crystal growth were slightly inferior to total urinary proteins (TUPs) from healthy subjects that are known to strongly inhibit COM stone formation. Surprisingly, its inhibitory effect against crystal aggregation was slightly superior to TUPs. While TUPs dramatically inhibited crystal-cell adhesion, CNB had no effect on this process. Ca^{2+}-affinity assay revealed that CNB strongly bound Ca^{2+} at a comparable degree as of TUPs. These findings indicate that CNB serves as a novel inhibitor of COM crystallization, growth and aggregation via its high Ca^{2+}-affinity property.

1. Introduction

Calcineurin is a protein phosphatase with Ca^{2+}- and calmodulin-dependent functions [1–3]. Its subunits A (CNA) and B (CNB) form a heterodimer as the functional structure [1,3]. CNA contains an enzyme catalytic domain, whereas CNB consists of four EF-hand domains that play roles in Ca^{2+}-binding [1]. Calcineurin has an important function in immune activation via dephosphorylation of nuclear factor of activated T cell (NFAT) [4,5]. The activated NFAT then translocates into nucleus and upregulates interleukin-2 (IL-2) (pro-inflammatory cytokine) production [4,5]. Hence, calcineurin serves as the primary target for a group of immunosuppressive drugs, namely calcineurin inhibitors (CNIs), which are widely used for preventing allograft rejection and prolonging the allograft half-life in organ transplantation [6,7]. Since the therapeutic window of CNIs is narrow, underdosage is associated with the high risk of allograft rejection, whereas overdosage frequently induces various toxicities, i.e., chronic allograft nephropathy, electrolyte imbalance and cardiovascular disorders [8–11].

Besides the canonical calcineurin-NFAT axis of signaling in the lymphoid cells, recent studies have demonstrated that CNIs, i.e., cyclosporin A (CsA) and tacrolimus (FK506), can induce toxicities in kidney epithelial cells via upregulation of tumor necrosis factor receptor superfamily, 12 A (TNFRSF12A) (alternatively, FN14, HPIP and TWEAKR) [12,13], which is independent of NFAT [12]. Another study has shown that a high proportion of the kidney-transplant patients who receive high-dose CNIs (CsA or FK506) exhibit hypocitraturia (69%) and hyperoxaluria (35%) [14]. Interestingly, some of them develop intrarenal calcium oxalate (CaOx) crystal deposition and urolithiasis (kidney stone disease) [14]. Additionally, a recent study has demonstrated that disruption of calcineurin signaling strongly affects transcriptome and proteome profiles of distal convoluted tubules, thereby affecting ion transports in this tubular segment of the kidney [10].

According to the molecular structure of calcineurin, CNB is the responsible subunit involved in Ca^{2+} homeostasis via Ca^{2+}/calmodulin complex [1]. CNB is found not only in the serum [15] but also in the urine [16]. Therefore, CNB is likely to affect Ca^{2+} balance in the tubulo-urinary system. From these backgrounds, we hypothesized that CNIs suppress activities of calcineurin (their primary target) in urinary

* Correspondence to: Head of Medical Proteomics Unit, Research Department, Siriraj Hospital, Mahidol University, 6th Floor - SiMR Building, 2 Wanglang Road, Bangkoknoi, Bangkok 10700, Thailand.
E-mail addresses: thongboonkerd@dr.com, vthongbo@yahoo.com (V. Thongboonkerd).

https://doi.org/10.1016/j.csbj.2023.07.038
Received 7 May 2023; Received in revised form 30 July 2023; Accepted 30 July 2023
Available online 31 July 2023

passage, leading to increased risk of kidney stone formation in CNIs-treated transplant patients. And CNB may serve as a stone inhibitor. Therefore, this study aimed to investigate effects of CNB on kidney stone formation using CaOx monohydrate (COM), a major pathogenic crystal in kidney stones, as an in vitro study model.

2. Materials and methods

2.1. Calcineurin sequence and structure analyses

Protein sequences of human calcineurin subunit A (CNA), α isoform (Q08209 with 512 amino acid residues), β isoform (P16298 with 524 residues) and γ isoform (P48454 with 512 residues) and human calcineurin subunit B (CNB), α isoform (P63098 with 170 residues) and β isoform (Q96LZ3 with 170 residues) from the UnitProtKB/Swiss-Prot database (*https://www.uniprot.org/uniprotkb*) were subjected to sequence and structure analyses. Three-dimensional structures of these sequences were predicted by AlphaFold Protein Structure Database (*www.alphafold.ebi.uk*). The sequence analysis was done by using CAPS tool (Coevolution Analysis using Protein Sequences) (*http://bioinf.gen.tcd.ie/~faresm/software/software.html*), RaptorX web server (*http://raptorx6.uchicago.edu/*), and ScanProsite tool (*https://prosite.expasy.org/scanprosite/*). Thereafter, the specific domains and/or patterns were crosschecked using ProRule (*https://prosite.expasy.org/prorule.html*). Graphical illustration of EF-hand (Ca^{2+}-binding) domains in the CNB molecule was generated by using SWISS-MODEL (*https://swissmodel.expasy.org/*) and UCSF ChimeraX software (version 1.3) (*https://www.rbvi.ucsf.edu/chimerax*).

2.2. Chemical preparation

Calcium chloride ($CaCl_2{\cdot}2\ H_2O$) (Merck; Branchburg, NJ) was prepared at 10 mM in crystallization buffer, which contains 10 mM Tris (Affymetrix inc.; Cleverland, OH) and 90 mM sodium chloride (NaCl) (Bio Basic; Toronto, Canada) (pH 7.4). Sodium oxalate ($Na_2C_2O_4$) (Sigma-Aldrich; St. Louis, MO) was also prepared at 1 mM in the crystallization buffer. Recombinant human calcineurin B (CNB) (Abcam; Cambridge, UK) and lysozyme (Sigma-Aldrich) were solubilized in the crystallization buffer at 1 mg/ml.

2.3. Preparation of total urinary proteins (TUPs)

TUPs were prepared from healthy subjects as described previously [17]. The study protocol met the standard guidelines (Declaration of Helsinki, Belmont Report, and ICH Good Clinical Practice) and was approved by Siriraj Institutional Review Board (approval no. Si473/2015). Briefly, mid-stream urine samples were collected from healthy subjects and clarified by centrifugation at 1000 *g* and 4 °C for 10 min to remove precipitants, debris and/or particles. The pooled clarified urine was then dialyzed with deionized water overnight at 4 °C and lyophilized. The dried TUPs were suspended in the crystallization buffer, and their final concentration were adjusted at 1 mg/ml.

2.4. Crystallization assay

Crystallization assay was performed following protocol described in previous studies [18,19]. In brief, 500 μl of 10 mM $CaCl_2{\cdot}2\ H_2O$ in the crystallization buffer was put into each well of 24-well plate (Corning Inc.; Corning, NY). Then, 4 μl of 1 mg/ml recombinant human CNB, 1 mg/ml TUPs, 1 mg/ml lysozyme (negative control), or crystallization buffer without any protein added (blank control) was added, followed by 500 μl of 1 mM $Na_2C_2O_4$. The mixture was incubated at 25 °C for 60 min, and the resulting COM crystals were imaged using an inverted light microscope (Eclipse Ti-S; Nikon; Tokyo, Japan). Crystal size and number were measured from at least 100 crystals in 10 random fields per sample using NIS-element D software version 4.11 (Nikon). Crystal abundance was then calculated.

$$\textit{Crystal abundance } (\mu m^2/\textit{field}) = \textit{Average crystal area in each field } (\mu m^2) \times \textit{Number of crystals in each field (/field)} \quad (1)$$

2.5. Crystal growth assay

Crystal growth assay was performed following protocol described in previous studies [20,21]. In brief, 500 μl of 10 mM $CaCl_2{\cdot}2\ H_2O$ in the crystallization buffer was put into each well of 24-well plate (Corning Inc.), followed by 500 μl of 1 mM $Na_2C_2O_4$. The mixture was incubated at 25 °C for 60 min. At this time-point (T_0), 4 μl of 1 mg/ml recombinant human CNB, 1 mg/ml TUPs, 1 mg/ml lysozyme (negative control), or crystallization buffer without any protein added (blank control) was added, followed by another incubation at 25 °C for 60 min (T_{60}). At T_0 and T_{60}, COM crystals were imaged using an inverted light microscope (Eclipse Ti-S). Crystal size was measured from at least 100 crystals in 10 random fields per sample using NIS-element D software version 4.11 (Nikon). Δ Area and crystal inhibitory activity were then calculated.

$$\Delta\ \textit{Area } (\mu m^2) = \textit{Crystal size at } T_{60}\ (\mu m^2) - \textit{Crystal size at } T_0\ (\mu m^2) \quad (3)$$

$$\textit{Crystal growth inhibitory activity } (\%) = ((\Delta\ \textit{Area of blank control} - \Delta\ \textit{Area of sample}) / \Delta\ \textit{Area of blank control}) \times 100 \quad (4)$$

2.6. Crystal aggregation assay

Crystal aggregation assay was performed following protocol described in previous studies [22,23]. In brief, 10 mM $CaCl_2{\cdot}2\ H_2O$ was mixed 1:1 with 1 mM $Na_2C_2O_4$, and the mixture was incubated overnight at 25 °C. The resulting COM crystals were harvested by centrifugation at 2000 *g* for 5 min, washed with methanol thrice and air-dried overnight at 25 °C. An equal amount of COM crystals (1000 μg) was suspended in 1 ml of crystallization buffer in each well of 6-well plate (Corning Inc.), followed by 4 μl of 1 mg/ml recombinant human CNB, 1 mg/ml TUPs, 1 mg/ml lysozyme (negative control), or crystallization buffer without any protein added (blank control). The plate was continuously shaken in a shaking incubator (Zhicheng; Shanghai, China) for 1 h at 150 rpm and 25 °C. The resulting crystal aggregates (each has been defined as "an assembly of three or more individual COM crystals that tightly joined together" [22]) were imaged using an inverted light microscope (Eclipse Ti-S). Number of the crystal aggregates was counted from at least 15 random fields per sample.

2.7. Crystal-cell adhesion assay

Crystal-cell adhesion assay was performed following protocol described in previous studies [24,25]. In brief, COM crystals were prepared and harvested as described above in the crystal aggregation assay. After air-dry, the crystals were decontaminated by UV light radiation for 30 min. MDCK renal cells (ATCC; Manassas, VA) were seeded and grown in each well of the 6-well plate (2×10^5 cells/well) for 48 h to obtain confluent monolayer. The culture supernatant was replaced with the fresh medium containing COM crystals (100 μg/ml) with 4 μl of 1 mg/ml recombinant human CNB, 1 mg/ml TUPs, 1 mg/ml lysozyme (negative control), or crystallization buffer without any protein added (blank control). The cells were further incubated for 1 h, followed by vigorous washes with PBS to remove the non-adhered crystals. The remaining crystals on the cell surface were imaged using an inverted light microscope (Eclipse Ti-S) and counted from at least 15 random fields per sample.

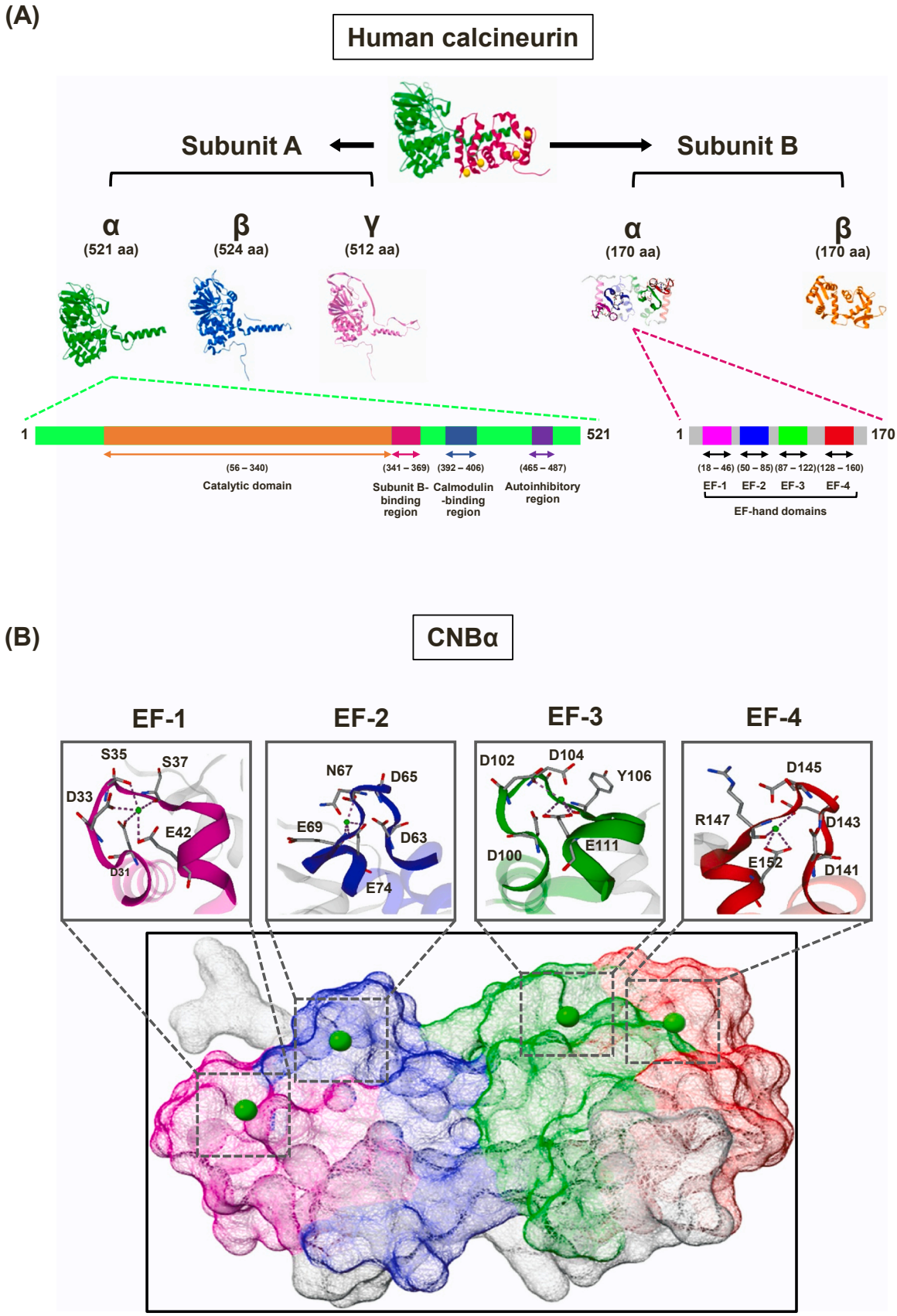

Fig. 1. Calcineurin sequence and structure analyses. **(A):** Calcineurin is a heterodimer comprising subunits A (CNA) and B (CNB). CNA is a catalytic subunit containing three isoforms (α, β and γ). Each of these isoforms consists of (i) catalytic domain, (ii) subunit B-binding region, (iii) calmodulin-binding region, and (iv) autoinhibitory region. CNB is a regulatory subunit containing two isoforms (α and β), each of which consists of four EF-hand (Ca^{2+}-binding) domains. **(B):** Key residues in each EF-hand domain of CNB (using CNBα isoform as a representative to illustrate).

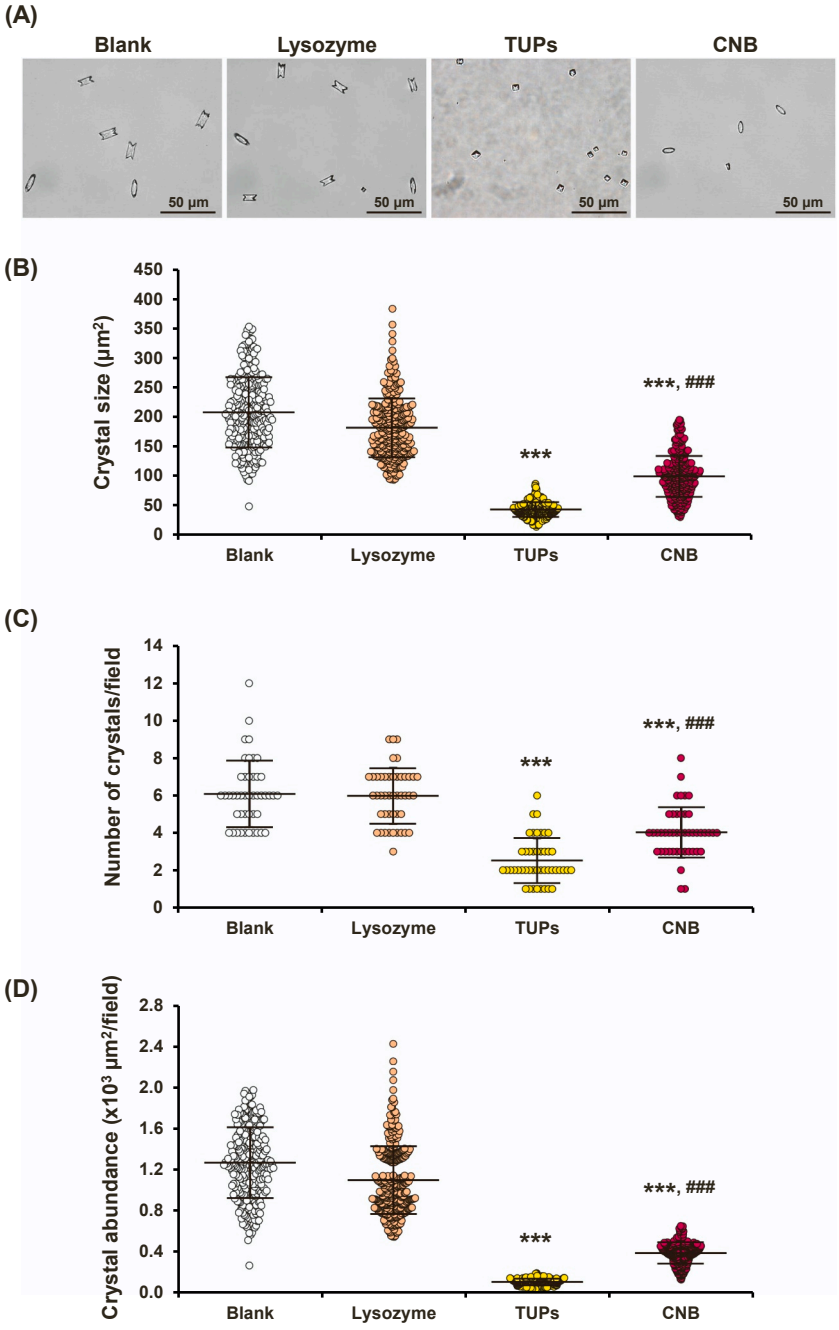

Fig. 2. Crystallization assay. During the assay, 4 μl of 1 mg/ml recombinant human CNB, 1 mg/ml TUPs, 1 mg/ml lysozyme (negative control), or crystallization buffer without any protein added (blank control). **(A):** COM crystal morphology under an inverted light microscope. **(B)-(D):** Crystal size, number and abundance were measured from at least 100 crystals in 10 random fields per sample using NIS-element D software version 4.11 (Nikon). The data were derived from three independent experiments using different samples and are reported as mean ± SD. * ** = P < 0.0001 vs. blank control; ### = P < 0.0001 vs. TUPs.

2.8. Ca^{2+}-affinity assay

Ca^{2+}-affinity assay was performed following protocol described in previous studies [24,25]. Each well of the 96-well polystyrene microplate (Corning Inc.) was immobilized with 0.32 μg recombinant human CNB, TUPs, or lysozyme (negative control) solubilized in 100 μl coating buffer (15 mM Na_2CO_3 and 30 mM $NaHCO_3$; pH 9.6), or 100 μl coating buffer without any protein added (blank control) at 4 °C overnight. A total of three microplates were employed in this assay. After immobilization, the buffer was removed, and each well was washed with PBS thrice, added with 80 μl of 0.1 mM $CaCl_2{\cdot}2\,H_2O$, and incubated at 25 °C for 60 min. The starting (T_0) and remaining (T_{60}) [Ca^{2+}] in each well were measured by a Ca^{2+}-binding colorimetric assay using Arsenazo III reagent (BioSystems S.A.; Barcelona, Spain) [26,27]. Ca^{2+} consumption, which determines Ca^{2+}-affinity, was then calculated.

$$Ca^{2+}\ consumption\ (\%) = (([Ca^{2+}]_{T0} - [Ca^{2+}]_{T60}) / [Ca^{2+}]_{T0}) \times 100 \quad (4)$$

Where $[Ca^{2+}]_{T0}$ was $[Ca^{2+}]$ at starting point before incubation with the protein, and $[Ca^{2+}]_{T60}$ was the remaining $[Ca^{2+}]$ after 60-min incubation with the protein.

2.9. Statistical analysis

All assays were performed in three independent experiments using different samples and are reported as mean ± SD. Multiple comparisons were performed using one-way analysis of variance (ANOVA) with Tukey's post-hoc test. *P* value less than 0.01 was set as the significant threshold in this study.

3. Results

Using the UnitProtKB/Swiss-Prot database, calcineurin showed two

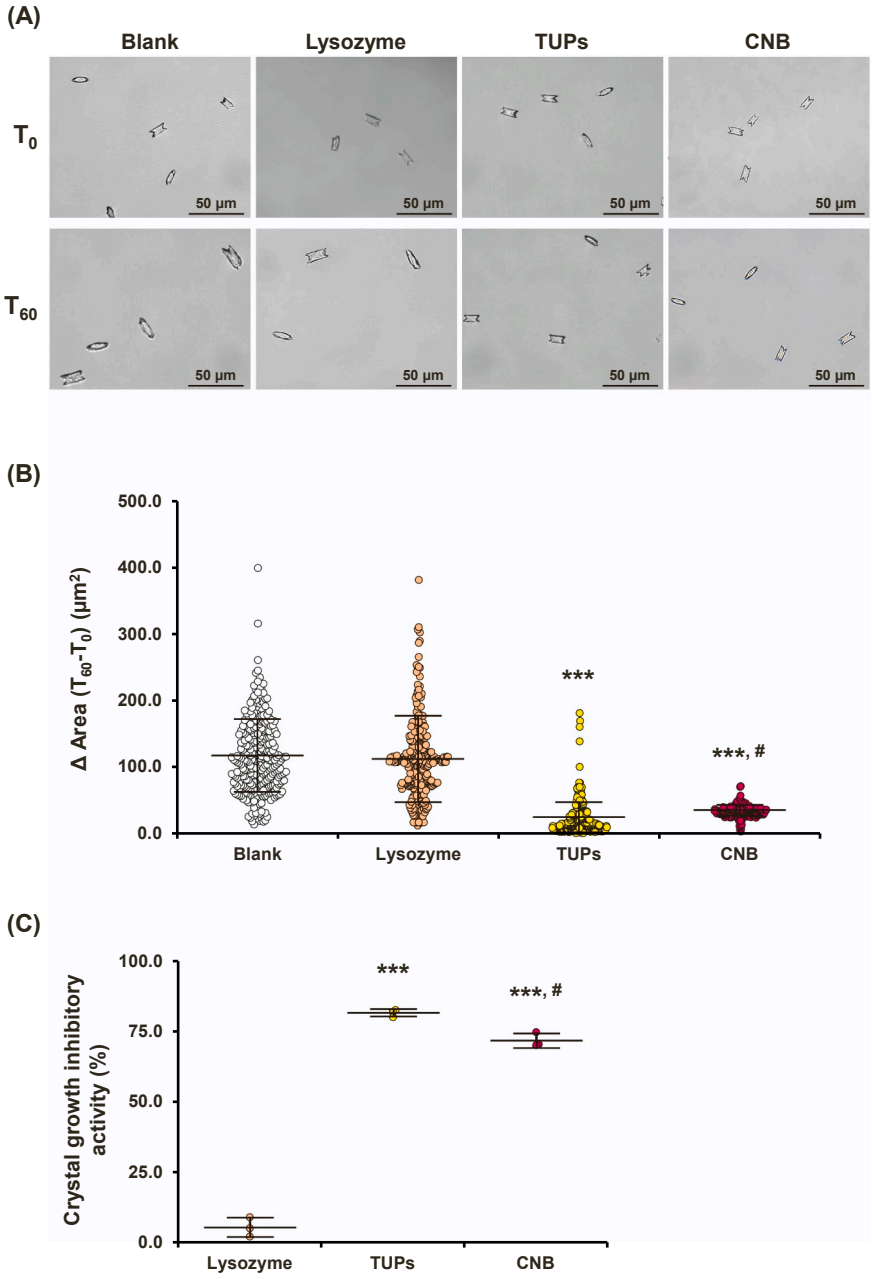

Fig. 3. Crystal growth assay. During the assay, 4 μl of 1 mg/ml recombinant human CNB, 1 mg/ml TUPs, 1 mg/ml lysozyme (negative control), or crystallization buffer without any protein added (blank control). **(A):** At T_0 and T_{60}, COM crystals were imaged using an inverted light microscope. **(B) and (C):** Δ Area and crystal growth inhibitory activity were calculated from at least 100 crystals in 10 random fields per sample using NIS-element D software version 4.11 (Nikon). The data were derived from three independent experiments using different samples and are reported as mean ± SD. * ** = $P < 0.0001$ vs. blank control; # = $P < 0.01$ vs. TUPs.

main subunits, CNA and CNB, to form a heterodimer (Fig. 1A). Sequence and structure analyses revealed that CNA is a catalytic subunit containing three isoforms (α, β and γ). Each of these isoforms consists of (i) catalytic domain, (ii) subunit B-binding region, (iii) calmodulin-binding region, and (iv) autoinhibitory region. CNB is a regulatory subunit containing two isoforms (α and β), each of which consists of four EF-hand (Ca^{2+}-binding) domains (Fig. 1A). Key amino acid residues responsible for Ca^{2+}-binding in each of these EF-hand domains of CNB (α isoform, as the representative) are illustrated in Fig. 1B. Therefore, it is likely that CNB affects COM crystals and may serve as a novel stone inhibitor.

Crystallization assay was employed to validate the effects of CNB on COM crystallization using lysozyme as the negative control. The results demonstrated that total urinary proteins (TUPs) from healthy subjects, that are known to strongly inhibit COM stone formation [17], markedly reduced COM crystal size, number and abundance comparing with blank and negative controls (Fig. 2). Also, CNB markedly reduced COM crystal size, number and abundance as compared with blank and negative controls. Comparing with TUPs, the inhibitory effects from CNB were slightly inferior to those from TUPs (Fig. 2).

Effects of CNB on COM crystal growth were then examined. After the crystals formed (T_0), the crystals were further incubated with CNB, TUPs, lysozyme (negative control), or crystallization buffer without any protein added (blank control) for 60 min (T_{60}). The crystal growth (as determined by Δ area of crystal size at T_{60} versus T_0) and crystal growth inhibitory activity were determined. As expected, TUPs markedly reduced Δ area comparing with blank and negative controls (Fig. 3). As a result, TUPs had a much greater crystal growth inhibitory activity as compared with the negative control (lysozyme). Similarly, CNB obviously reduced Δ area as compared with blank and negative controls, and had a much greater crystal growth inhibitory activity comparing with the negative control. Between TUPs and CNB, the inhibitory effects of CNB were slightly inferior to those of TUPs (Fig. 3).

Crystal aggregation assay was employed to investigate the effects of

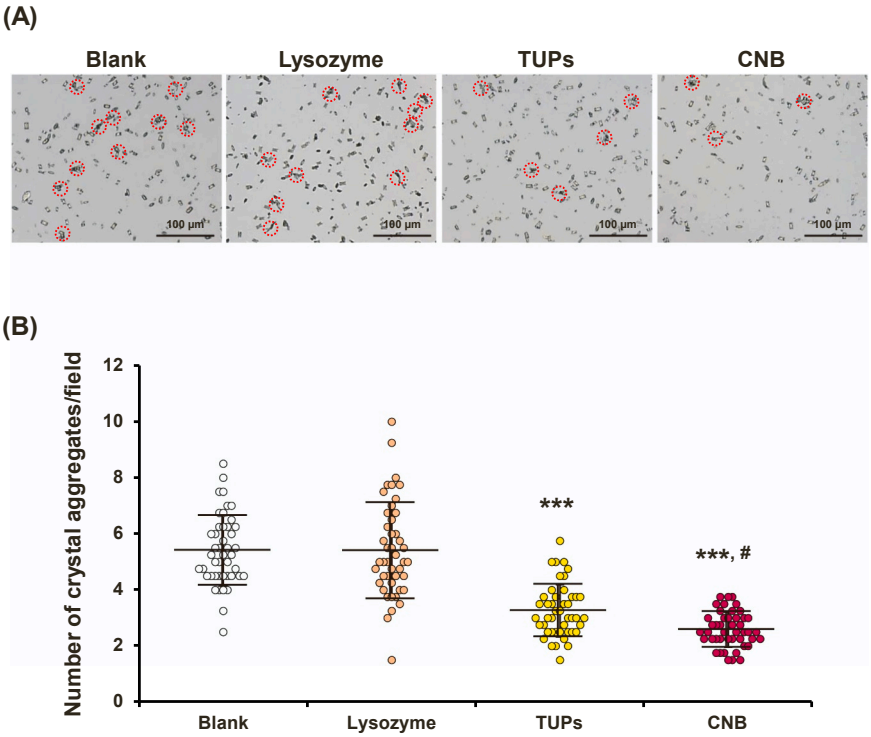

Fig. 4. Crystal aggregation assay. During the assay, 4 μl of 1 mg/ml recombinant human CNB, 1 mg/ml TUPs, 1 mg/ml lysozyme (negative control), or crystallization buffer without any protein added (blank control). **(A):** The resulting crystal aggregates (each has been defined as "an assembly of three or more individual COM crystals that tightly joined together" [22]) were imaged using an inverted light microscope. **(B):** Number of the crystal aggregates was counted from at least 15 random fields per sample. The data were derived from three independent experiments using different samples and are reported as mean ± SD. * ** = $P < 0.0001$ vs. blank control; # = $P < 0.01$ vs. TUPs.

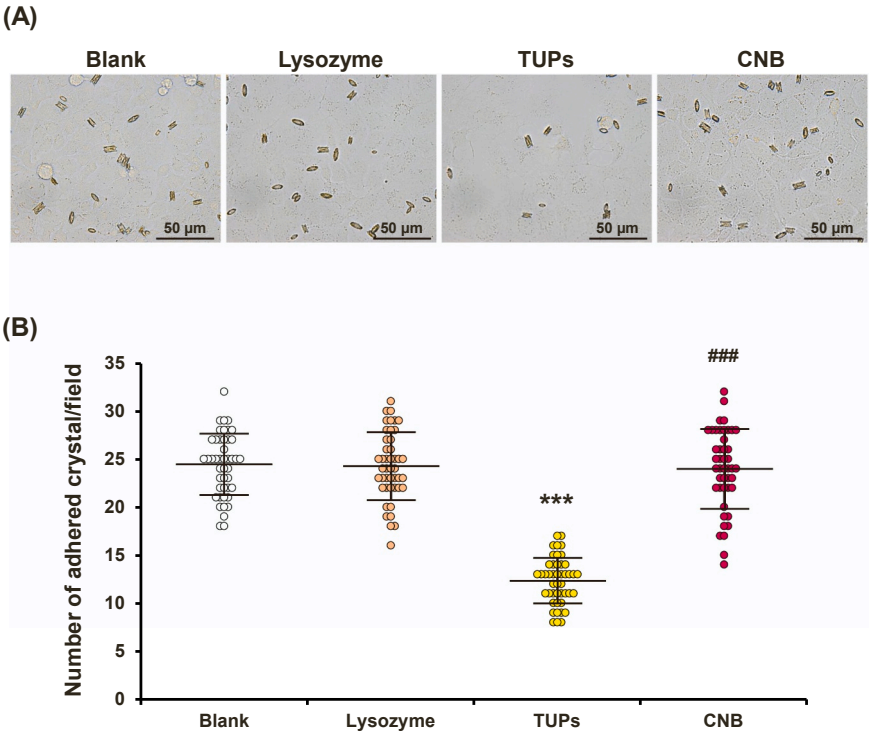

Fig. 5. Crystal-cell adhesion assay. During the assay, 4 μl of 1 mg/ml recombinant human CNB, 1 mg/ml TUPs, 1 mg/ml lysozyme (negative control), or crystallization buffer without any protein added (blank control). **(A):** The remaining crystals on the cell surface were imaged using an inverted light microscope. **(B):** Number of the remaining crystals was counted from at least 15 random fields per sample. The data were derived from three independent experiments using different samples and are reported as mean ± SD. * ** = $P < 0.0001$ vs. blank control; ### = $P < 0.0001$ vs. TUPs.

CNB on COM crystal aggregation. The data showed that TUPs significantly decreased number of COM crystal aggregates comparing with blank and negative controls (Fig. 4). Also, CNB significantly decreased number of COM crystal aggregates comparing with blank and negative controls. Surprisingly, the degree of inhibitory effects of CNB on crystal aggregation was slightly superior to that of TUPs (Fig. 4).

Crystal-cell adhesion assay was conducted by measuring number of the remaining crystals on the cell surfaces after incubation and vigorous washes. The data demonstrated that TUPs markedly decreased number of the remaining crystals adhered on the cell surfaces comparing with blank and negative controls (Fig. 5). However, CNB had no significant effects on COM crystal-cell adhesion comparing with blank and negative controls (Fig. 5).

To define mechanism underlying the inhibitory effects of CNB on

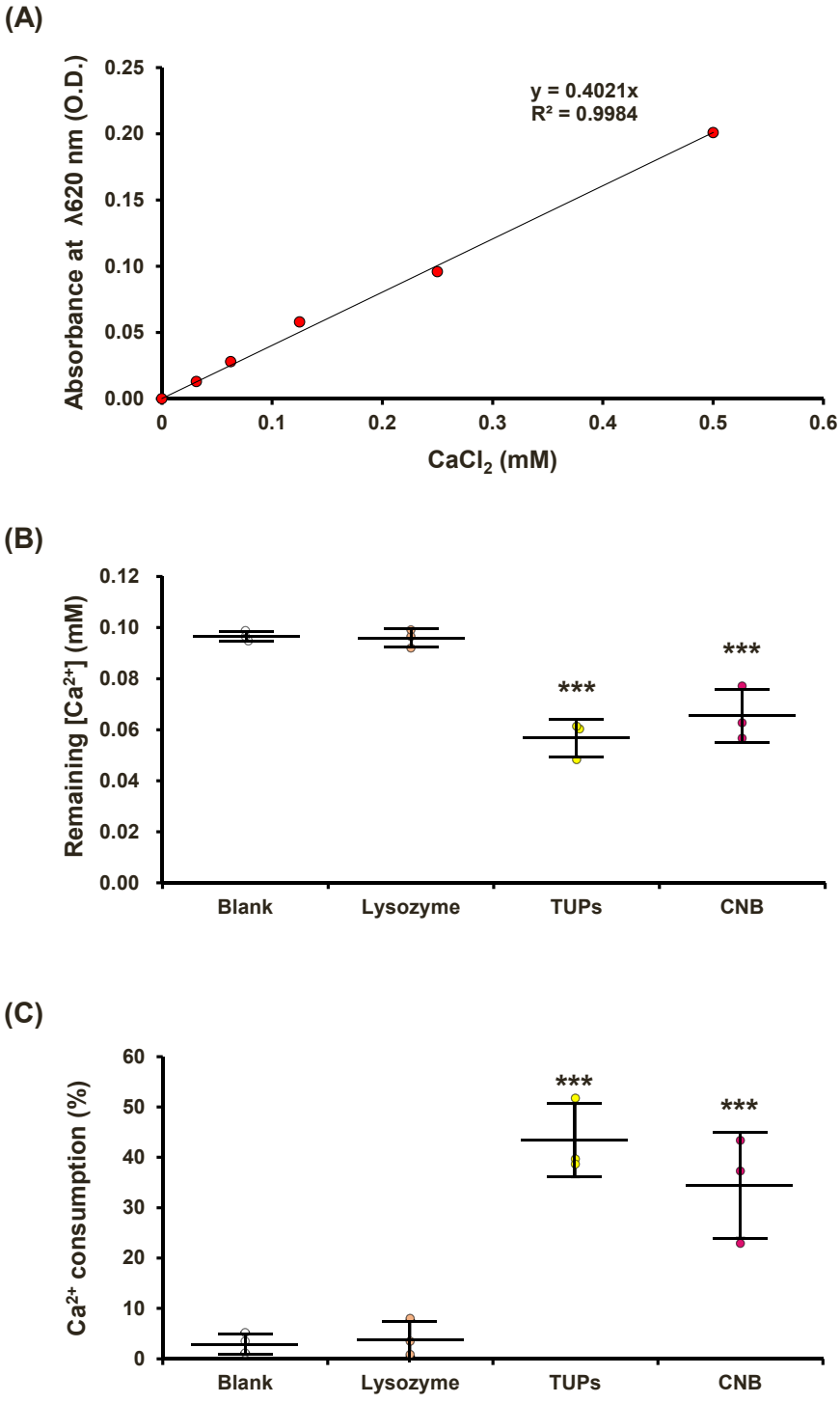

Fig. 6. Ca^{2+}-affinity assay. Equal amount of recombinant human CNB, TUPs or lysozyme (negative control) in coating buffer, or equal volume of coating buffer without any protein added (blank control) was immobilized in each well of a microplate and incubated with 0.1 mM $CaCl_2{\cdot}2\ H_2O$ at 25 °C for 60 min **(A):** The standard curve of $[Ca^{2+}]$ measured by Ca^{2+}-binding colorimetric assay using Arsenazo III reagent. **(B):** The starting (T_0) and remaining (T_{60}) $[Ca^{2+}]$ in each well were then measured using Arsenazo III reagent and the standard curve. **(C):** Ca^{2+} consumption, which determines Ca^{2+}-affinity, was then calculated. The data were derived from three independent experiments using different samples and are reported as mean ± SD. * ** = $P < 0.0001$ vs. blank control.

COM crystals, Ca^{2+}-affinity assay was performed. The standard curve of $[Ca^{2+}]$ measured by Arsenazo III reaction of $CaCl_2{\cdot}2\ H_2O$ at 0, 0.0312, 0.0625, 0.1250, 0.2500 and 0.5000 mM was constructed to be used for measurement of the remaining $[Ca^{2+}]$ in the samples after Ca^{2+}-affinity for 60 min ($R^2 = 0.9968$) (Fig. 6A). Obvious decrease of the remaining $[Ca^{2+}]$ was detected in both TUPs and CNB samples (Fig. 6B), due to the high-degree of Ca^{2+} consumption in both TUPs and CNB as compared with blank and negative controls (Fig. 6C). There were no significance differences in the remaining $[Ca^{2+}]$ and Ca^{2+} consumption between TUPs and CNB found (Fig. 6B and C).

4. Discussion

Calcineurin is a cytosolic Ca^{2+}/calmodulin-dependent enzyme that plays roles in dephosphorylation process [28]. This protein phosphatase regulates gene expression dependently on the change in $[Ca^{2+}]$ [28]. Its heterodimer consists of CNA (calmodulin-binding catalytic subunit) and CNB (Ca^{2+}-binding regulatory subunit) [1]. Calcineurin activation occurs when intracellular $[Ca^{2+}]$ increases and binds to the Ca^{2+}-binding sites of the CNB regulatory subunit [29]. Thereafter, the Ca^{2+} load of CNB induces a conformational change of the CNA subunit, which then promotes Ca^{2+}/calmodulin interaction and activates downstream

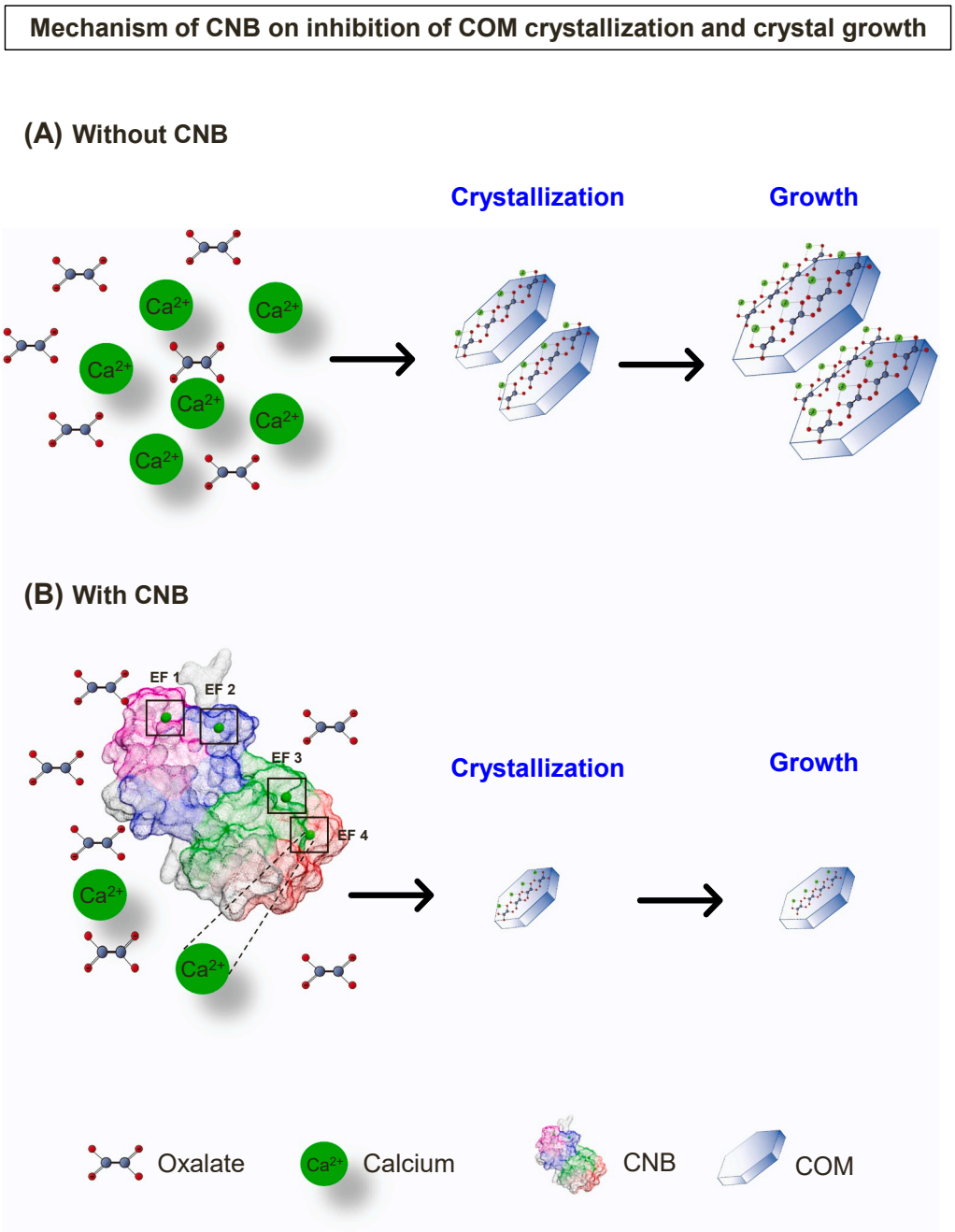

Fig. 7. Mechanism of CNB on inhibition of COM crystallization and crystal growth. **(A):** COM crystals are formed by Ca^{2+} and oxalate ions in the supersaturated urine or renal tubular fluid. After crystallization, the free Ca^{2+} and oxalate ions can add onto crystalline surfaces, leading to crystal growth. **(B):** In the presence of CNB in the urine, the free Ca^{2+} ions are captured by EF-hand (Ca^{2+}-binding) domains in the CNB molecules, leading significant decrease in free Ca^{2+} ions, which are crucial for COM crystal formation and growth, leading to inhibition of COM crystallization and crystal growth.

signaling [29]. During immune responses, intracellular [Ca^{2+}] increases with repetitive and prolonged Ca^{2+} influx, leading to calcineurin activation and dephosphorylation of NFAT [4,5]. Consequently, the activated NFAT translocates to the nucleus and upregulates proinflammatory cytokine (IL-2) production [4,5]. Thus, the activated calcineurin is a key mediator of immune regulation. For this reason, calcineurin serves as a main target for the immunosuppressants known as calcineurin inhibitors (CNIs), which are widely used in solid organ transplantation [12].

Although effective, CNIs treatment is strongly associated with many complications, such as hypertension and electrolyte imbalance (e.g., hyperkalemia, hypomagnesemia, metabolic acidosis, and hypercalciuria) [6]. Previous reports have shown that patients, who underwent kidney transplantation and receive CNIs (CsA or FK506), have abnormal urinary profiles, hypocitraturia and hyperoxaluria [6,9,30,31]. As hypercalciuria, hypocitraturia and hyperoxaluria are among the major risks for CaOx urolithiasis [32], CNIs thus increase the risk for CaOx stone development. Additionally, a recent study has shown that FK506 affects transportation of magnesium and Ca^{2+} along the distal convoluted tubules in mice [33]. This type of CNIs induces hypomagnesemia and hypercalciuria by reducing mRNA and protein expression of the responsible ion transporters [33]. The increased risk of urolithiasis has been confirmed in a study of 53 successful kidney-transplant children who receive CsA or FK506, revealing crystal deposition and urolithiasis in some of these patients [14].

We thus hypothesized that the Ca^{2+}-binding subunit of calcineurin (CNB), which is the target of CNIs, should play roles in CaOx kidney stone formation (likely to be an inhibitor, in an opposite direction as of CNIs, which seem to be the promotor). The study was conducted using various COM crystal assays. Our results demonstrated that CNB contains four EF-hand Ca^{2+}-binding domains. Crystallization assay showed that CNB significantly inhibited COM crystal formation and growth with a

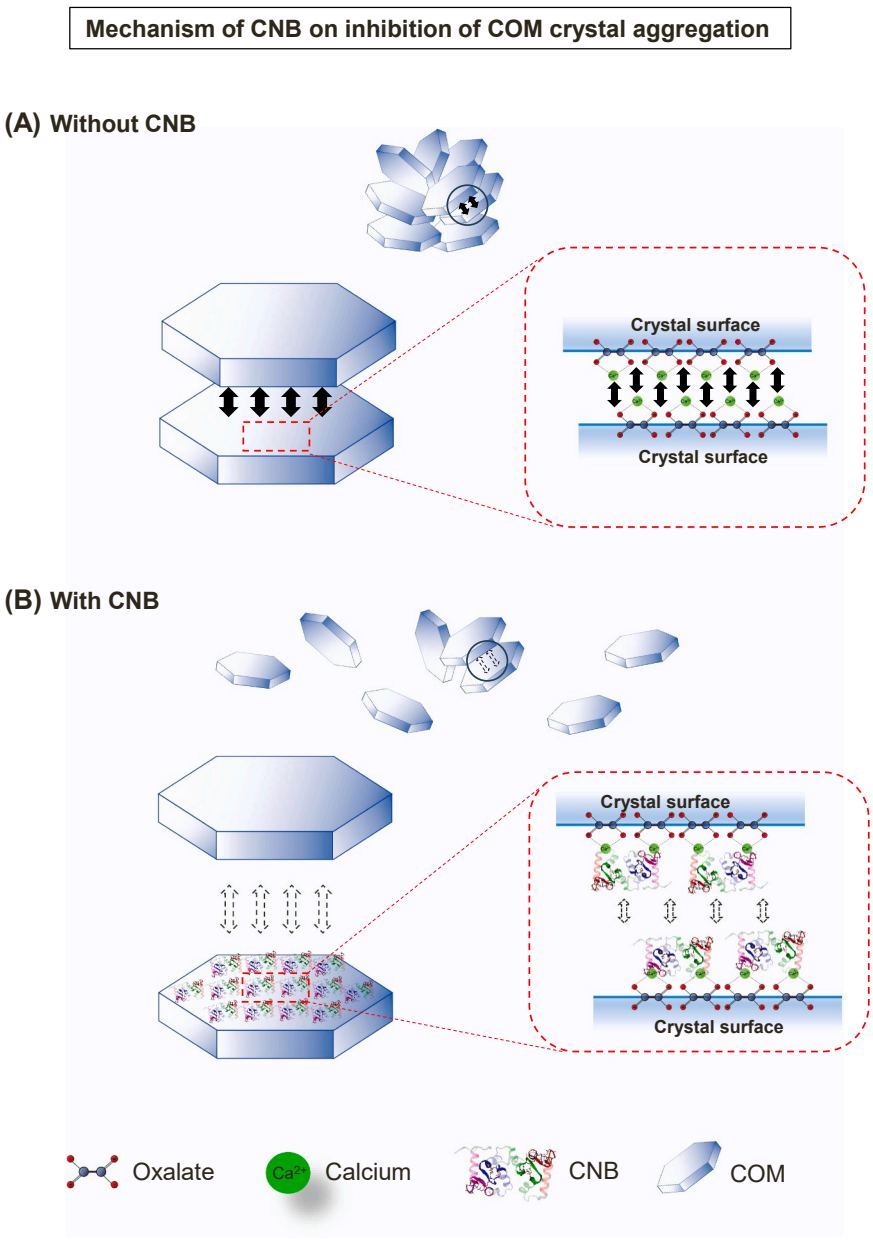

Fig. 8. Mechanism of CNB on inhibition of COM crystal aggregation. **(A):** COM crystals generally have a high adhesive capability that can bind to various surfaces, including the crystal surfaces themselves, leading to crystal self-aggregation. **(B):** In the presence of CNB in the urine, CNB can bind to the crystal surfaces rich with Ca^{2+} molecules via EF-hand (Ca^{2+}-binding) domains, thereby reducing adhesive force on the crystal surfaces, leading to inhibition of crystal aggregation.

slightly less potency as of TUPs, the known natural stone inhibitors. Additionally, CNB significantly inhibited COM crystal aggregation with a slightly greater potency as of TUPs. While TUPs significantly inhibited COM crystal-cell adhesion, CNB did not affect this stone formation step. Ca^{2+}-affinity assay revealed obvious decrease of the remaining [Ca^{2+}] in CNB samples after Ca^{2+}-affinity for 60 min, comparable to that of TUPs. The data also showed approximately 40% Ca^{2+} consumption by both CNB and TUPs, indicating that the inhibitory effects of CNB and TUPs against COM crystals were mediated via their Ca^{2+}-binding properties.

Kidney stone development is a sophisticated event that can be initiated from crystal nucleation, followed by continuous accumulation of crystal components to the crystal seed (leading to crystal growth), crystal aggregation, and crystal-cell adhesion [34,35]. In general, kidney stone formation requires several factors for its initiation. For the most common stone type, CaOx crystals are formed by Ca^{2+} and oxalate ions in the supersaturated urine or renal tubular fluid [36]. CNB is modified by myristoylation and predominantly localizes intracellularly at the inner membrane leaflets [37]. Interestingly, CNB is also excreted into the urine [16]. Based on its Ca^{2+}-binding capability and excretion, it is likely to inhibit CaOx crystal formation, growth and aggregation, and thus neutralize the stone-promoting effects induced by CNIs.

Crystal adhesion on apical membranes of renal cells is one of the key steps in kidney stone formation as it promotes crystal retention in the kidney [38]. The longer that the crystals retain, the higher chance of kidney stone to develop. The retained crystals can further enlarge by urinary supersaturation of Ca^{2+} and oxalate ions [39]. Additionally, the retained crystals can promote renal epithelial cell injury, one of the risk factors for urolithiasis [39,40]. Our present study, however, showed no effects of CNB on crystal-cell adhesion. Generally, adhesion of intact crystal particles to the renal epithelial cells requires receptors or receptor-like molecules [25,41,42]. In addition, COM crystals that contain Ca^{2+}-rich ($1\bar{0}1$) active face easily adhere to the cells [43]. Although the Ca^{2+}-affinity ability of CNB could reduce crystal formation, growth and aggregation, such property might not interfere with the

surface property of the crystals and their receptors on the cell membranes.

In addition to crystal-cell adhesion, crystallization, crystal growth and crystal aggregation are the other key steps for kidney stone formation [44,45]. Our present study demonstrated that while CNB did not affect crystal-cell adhesion, it strongly inhibited COM crystal formation, growth and aggregation. The proposed mechanisms of CNB on inhibition of COM crystal formation, growth and aggregation are summarized in Figs. 7 and 8. These effects would dramatically reduce the starting inorganic stone materials, thereby inhibiting the stone formation.

It should be also noted that TUPs contain a large number of proteins [46,47], each of which may or may not have the stone modulatory activity [48]. The effects of TUPs on the stone modulation would be a result of the average effects from all the proteins present in the urine. Comparing with numerous other urinary proteins, CNB represents only a very tiny fraction of the TUPs. Therefore, the effects of other urinary proteins should be also taken into account for the inhibitory effects of TUPs observed in our present study. Additionally, the equal amount of proteins (4 μl of each protein at a concentration of 1 mg/ml) was used for evaluating their modulatory activities on COM crystals in a total volume of 1 ml in each assay. This amount/concentration was entirely based on the standard protocol established for the crystal assays to evaluate in vitro COM stone formation processes. Therefore, translation of these data to the clinic would require evaluation of their urinary concentrations and validation of their effects in humans.

In summary, our present study revealed that CNB dramatically inhibited COM crystal formation, growth and aggregation. At an equal amount, degrees of its inhibition against crystallization and crystal growth were slightly inferior to that of TUPs from healthy subjects that are known to strongly inhibit COM stone formation. Surprisingly, its inhibitory effect against crystal aggregation was slightly superior to that of TUPs. While TUPs dramatically inhibited crystal-cell adhesion, CNB had no effect on this process. Ca^{2+}-affinity assay revealed that CNB strongly bound Ca^{2+} at a comparable degree as of TUPs. These findings indicate that CNB serves as a novel inhibitor of COM crystallization, growth and aggregation via its high Ca^{2+}-affinity property.

CRediT authorship contribution statement

Sudarat Hadpech, Sakdithep Chaiyarit and Visith Thongboonkerd designed research; Sudarat Hadpech and Sakdithep Chaiyarit performed experiments; Sudarat Hadpech, Sakdithep Chaiyarit and Visith Thongboonkerd analyzed data; Sudarat Hadpech and Visith Thongboonkerd wrote the manuscript; All authors reviewed and approved the manuscript.

Declaration of Competing Interest

The authors declare that they have no known competing financial interests or personal relationships that could have appeared to influence the work reported in this paper.

Acknowledgements

We are grateful to Paleerath Peerapen, Sunisa Yoodee, and Supatcha Sassanarakkit for their technical assistance. This study was supported by the National Research Council of Thailand (NRCT): High-Potential Research Team Grant Program (N42A660625).

References

[1] Creamer TP. Calcineurin. Cell Commun Signal 2020;18:137.
[2] Li H, Hogan PG. Calcineurin: A star is reborn. Cell Calcium 2021;94:102324.
[3] Cook EC, Creamer TP. Calcineurin in a crowded world. Biochemistry 2016;55:3092–101.
[4] Xu XP, Yao YM, Zhao GJ, Wu ZS, Li JC, Jiang YL, et al. Role of the ca(2+)-calcineurin-nuclear factor of activated t cell pathway in mitofusin-2-mediated immune function of jurkat cells. Chin Med J (Engl) 2018;131:330–8.
[5] Bendickova K, Tidu F, Fric J. Calcineurin-nfat signalling in myeloid leucocytes: New prospects and pitfalls in immunosuppressive therapy. EMBO Mol Med 2017;9:990–9.
[6] Karolin A, Genitsch V, Sidler D. Calcineurin inhibitor toxicity in solid organ transplantation. Pharmacology 2021;106:347–55.
[7] Bauer AC, Franco RF, Manfro RC. Immunosuppression in kidney transplantation: State of the art and current protocols. Curr Pharm Des 2020;26:3440–50.
[8] Schiff J, Cole E, Cantarovich M. Therapeutic monitoring of calcineurin inhibitors for the nephrologist. Clin J Am Soc Nephrol 2007;2:374–84.
[9] Farouk SS, Rein JL. The many faces of calcineurin inhibitor toxicity-what the fk? Adv Chronic Kidney Dis 2020;27:56–66.
[10] Banki E, Fisi V, Moser S, Wengi A, Carrel M, Loffing-Cueni D, et al. Specific disruption of calcineurin-signaling in the distal convoluted tubule impacts the transcriptome and proteome, and causes hypomagnesemia and metabolic acidosis. Kidney Int 2021;100:850–69.
[11] Bentata Y. Tacrolimus: 20 years of use in adult kidney transplantation. What we should know about its nephrotoxicity. Artif Organs 2020;44:140–52.
[12] Karolin A, Escher G, Rudloff S, Sidler D. Nephrotoxicity of calcineurin inhibitors in kidney epithelial cells is independent of nfat signaling. Front Pharm 2021;12:789080.
[13] Claus M, Herro R, Wolf D, Buscher K, Rudloff S, Huynh-Do U, et al. The tweak/fn14 pathway is required for calcineurin inhibitor toxicity of the kidneys. Am J Transpl 2018;18:1636–45.
[14] Stapenhorst L, Sassen R, Beck B, Laube N, Hesse A, Hoppe B. Hypocitraturia as a risk factor for nephrocalcinosis after kidney transplantation. Pedia Nephrol 2005;20:652–6.
[15] Sankaranarayanan TK, Sethi BK, Subramanyam C. Serum calcineurin activity in relation to oxidative stress and glycemic control in type ii diabetes mellitus. Clin Biochem 2005;38:218–22.
[16] Swensen AC, He J, Fang AC, Ye Y, Nicora CD, Shi T, et al. A comprehensive urine proteome database generated from patients with various renal conditions and prostate cancer. Front Med (Lausanne) 2021;8:548212.
[17] Chaiyarit S, Thongboonkerd V. Oxidative modifications switch modulatory activities of urinary proteins from inhibiting to promoting calcium oxalate crystallization, growth, and aggregation. Mol Cell Proteom 2021;20:100151.
[18] Thongboonkerd V, Semangoen T, Chutipongtanate S. Factors determining types and morphologies of calcium oxalate crystals: Molar concentrations, buffering, ph, stirring and temperature. Clin Chim Acta 2006;367:120–31.
[19] Thongboonkerd V, Chutipongtanate S, Semangoen T, Malasit P. Urinary trefoil factor 1 is a novel potent inhibitor of calcium oxalate crystal growth and aggregation. J Urol 2008;179:1615–9.
[20] Amimanan P, Tavichakorntrakool R, Fong-ngern K, Sribenjalux P, Lulitanond A, Prasongwatana V, et al. Elongation factor tu on escherichia coli isolated from urine of kidney stone patients promotes calcium oxalate crystal growth and aggregation. Sci Rep 2017;7:2953.
[21] Khamchun S, Sueksakit K, Chaiyarit S, Thongboonkerd V. Modulatory effects of fibronectin on calcium oxalate crystallization, growth, aggregation, adhesion on renal tubular cells, and invasion through extracellular matrix. J Biol Inorg Chem 2019;24:235–46.
[22] Chaiyarit S, Thongboonkerd V. Defining and systematic analyses of aggregation indices to evaluate degree of calcium oxalate crystal aggregation. Front Chem 2017;5:113.
[23] Kanlaya R, Naruepantawart O, Thongboonkerd V. Flagellum is responsible for promoting effects of viable *escherichia coli* on calcium oxalate crystallization, crystal growth, and crystal aggregation. Front Microbiol 2019;10:2507.
[24] Peerapen P, Thongboonkerd V. Differential bound proteins and adhesive capabilities of calcium oxalate monohydrate crystals with various sizes. Int J Biol Macromol 2020;163:2210–23.
[25] Fong-ngern K, Sueksakit K, Thongboonkerd V. Surface heat shock protein 90 serves as a potential receptor for calcium oxalate crystal on apical membrane of renal tubular epithelial cells. J Biol Inorg Chem 2016;21:463–74.
[26] Chutipongtanate S, Thongboonkerd V. Establishment of a novel colorimetric assay for high-throughput analysis of calcium oxalate crystal growth modulation. Analyst 2010;135:1309–14.
[27] Noonin C, Peerapen P, Yoodee S, Kapincharanon C, Kanlaya R, Thongboonkerd V. Systematic analysis of modulating activities of native human urinary tamm-horsfall protein on calcium oxalate crystallization, growth, aggregation, crystal-cell adhesion and invasion through extracellular matrix. Chem Biol Inter 2022;357:109879.
[28] Sun B, Vaughan D, Tikunova S, Creamer TP, Davis JP, Kekenes-Huskey PM. Calmodulin-calcineurin interaction beyond the calmodulin-binding region contributes to calcineurin activation. Biochemistry 2019;58:4070–85.
[29] Ulengin-Talkish I, Cyert MS. A cellular atlas of calcineurin signaling. Biochim Biophys Acta Mol Cell Res 2023;1870:119366.
[30] Hoskova L, Malek I, Kopkan L, Kautzner J. Pathophysiological mechanisms of calcineurin inhibitor-induced nephrotoxicity and arterial hypertension. Physiol Res 2017;66:167–80.
[31] Issa N, Kukla A, Ibrahim HN. Calcineurin inhibitor nephrotoxicity: A review and perspective of the evidence. Am J Nephrol 2013;37:602–12.
[32] Youssef RF, Martin JW, Sakhaee K, Poindexter J, Dianatnejad S, Scales CD, et al. Rising occurrence of hypocitraturia and hyperoxaluria associated with increasing prevalence of stone disease in calcium kidney stone formers. Scand J Urol 2020;54:426–30.

[33] Gratreak BDK, Swanson EA, Lazelle RA, Jelen SK, Hoenderop J, Bindels RJ, et al. Tacrolimus-induced hypomagnesemia and hypercalciuria requires fkbp12 suggesting a role for calcineurin. Physiol Rep 2020;8:e14316.
[34] Rodgers AL. Physicochemical mechanisms of stone formation. Urolithiasis 2017; 45:27–32.
[35] Evan AP, Worcester EM, Coe FL, Williams Jr J, Lingeman JE. Mechanisms of human kidney stone formation. Urolithiasis 2015;43(Suppl 1):19–32.
[36] Xie B, Halter TJ, Borah BM, Nancollas GH. Aggregation of calcium phosphate and oxalate phases in the formation of renal stones. Cryst Growth Des 2015;15:204–11.
[37] Perrino BA, Martin BA. Ca(2+)- and myristoylation-dependent association of calcineurin with phosphatidylserine. J Biochem 2001;129:835–41.
[38] Wang Z, Zhang Y, Zhang J, Deng Q, Liang H. Recent advances on the mechanisms of kidney stone formation (review). Int J Mol Med 2021;48:149.
[39] Aggarwal KP, Narula S, Kakkar M, Tandon C. Nephrolithiasis: Molecular mechanism of renal stone formation and the critical role played by modulators. Biomed Res Int 2013;2013:292953.
[40] Williams Jr JC, McAteer JA. Retention and growth of urinary stones: Insights from imaging. J Nephrol 2013;26:25–31.
[41] Thongboonkerd V. Proteomics of crystal-cell interactions: A model for kidney stone research. Cells 2019;8:1076.
[42] Sheng X, Jung T, Wesson JA, Ward MD. Adhesion at calcium oxalate crystal surfaces and the effect of urinary constituents. Proc Natl Acad Sci USA 2005;102: 267–72.
[43] Sun XY, Xu M, Ouyang JM. Effect of crystal shape and aggregation of calcium oxalate monohydrate on cellular toxicity in renal epithelial cells. ACS Omega 2017; 2:6039–52.
[44] Peerapen P, Thongboonkerd V. Kidney stone prevention. Adv Nutr 2023.
[45] Chaiyarit S, Thongboonkerd V. Mitochondrial dysfunction and kidney stone disease. Front Physiol 2020;11:566506.
[46] Thongboonkerd V, McLeish KR, Arthur JM, Klein JB. Proteomic analysis of normal human urinary proteins isolated by acetone precipitation or ultracentrifugation. Kidney Int 2002;62:1461–9.
[47] Thongboonkerd V, Klein JB, Arthur JM. Proteomic identification of a large complement of rat urinary proteins. Nephron Exp Nephrol 2003;95:e69–78.
[48] Sassanarakkit S, Peerapen P, Thongboonkerd V. Stonemod: A database for kidney stone modulatory proteins with experimental evidence. Sci Rep 2020;10:15109.